Exact solutions for ice flow across the no-slip to free-slip transition

Journal:	*Journal of Glaciology*
Manuscript ID	JOG-2026-0074
Manuscript Type:	Article
Date Submitted by the Author:	20-May-2026
Complete List of Authors:	Moreno-Parada, Daniel; Universite Libre Bruxelles Faculte des Sciences, Laboratoire de Glaciologie Pattyn, Frank; Universite Libre Bruxelles Faculte des Sciences, Laboratoire de Glaciologie
Keywords:	Ice dynamics, Ice streams, Ice-sheet modelling
Abstract:	The downhill flow of a viscous ice stream across a no-slip to free-slip transition remains elusive to exact solutions due to the existence of singularities. Here we replace the point-wise sharp transition by a functional dependency of parametrised horizontal length. Analytical solutions are found for the steady Navier-Stokes flow with Newtonian properties. Our solution remains smooth and well-behaved across the entire domain. The upper surface deflection is observed if sliding is sufficiently reduced upstream of the transition. Ice flow overturning is possible under sharp basal transitions, illustrating that ice-core dating can be biased by the transition zone effect. The pressure singularity arises in the limit where the basal transition becomes discontinuous. Previous singular solutions are a result of a physically unrealistic domain definition. A simple ice-sheet–shelf junction is constructed from the analytical solutions, and admissible grounding line positions are identified by exploring a range of ice flux values. These solutions satisfy both contact inequalities for multiple flux values, demonstrating that equilibrium positions are not discrete, but rather form a continuos set of

	solutions. As a result, the grounding line position is not univocally determined by the ice flux in the linearised problem.

Exact solutions for ice flow across the no-slip to free-slip transition

Daniel MORENO-PARADA,[1,2] and Frank PATTYN,[1,2]

[1]*Laboratoire de Glaciologie, Université Libre de Bruxelles, Brussels, Belgium*

[2]*Brussels Laboratory of the Universe, BLU-ULB*

Correspondence: Daniel Moreno-Parada <daniel.moreno.parada@ulb.be>

ABSTRACT. The downhill flow of a viscous ice stream across a no-slip to free-slip transition remains elusive to exact solutions due to the existence of singularities. Here we replace the point-wise sharp transition by a functional dependency of parametrised horizontal length. Analytical solutions are found for the steady Navier-Stokes flow with Newtonian properties. Our solution remains smooth and well-behaved across the entire domain. The upper surface deflection is observed if sliding is sufficiently reduced upstream of the transition. Ice flow overturning is possible under sharp basal transitions, illustrating that ice-core dating can be biased by the transition zone effect. The pressure singularity arises in the limit where the basal transition becomes discontinuous. Previous singular solutions are a result of a physically unrealistic domain definition. A simple ice-sheet–shelf junction is constructed from the analytical solutions, and admissible grounding line positions are identified by exploring a range of ice flux values. These solutions satisfy both contact inequalities for multiple flux values, demonstrating that equilibrium positions are not discrete, but rather form a continuos set of solutions. As a result, the grounding line position is not univocally determined by the ice flux in the linearised problem.

INTRODUCTION

Ice discharge into the ocean is the main control of the Antarctic mass balance (Rignot and others, 2019). In marine regions, the rate of this discharge is governed by the transition where ice streams become afloat, and it represents more than 80% of the total outflow (Bamber and others, 2000; Pritchard and others, 2012). These so-called grounding zones are pivotal for reliable predictions of sea-level rise, as they capture the coupling between ice sheets and ice shelves. The complexity of grounding zones arises from the mechanical transition of two coexisting types of flow, where both shear and longitudinal stresses are relevant. The extent of these transition zones is not restricted to the exact flotation position, but rather covers a few ice thicknesses as longitudinal stresses propagate into the grounded ice sheet (Chugunov and Wilchinsky, 1996).

The first *ad hoc* results were obtained by Weertman (1974) with the aim of identifying viable grounding line equilibria. Chugunov and Wilchinsky (1996) and Wilchinsky and Chugunov (2001) then applied a matched asymptotic analysis to couple the grounded and floating parts of an ice sheet assuming a steady grounding line position. Fowler (2011) later arrived to a similar formulation, relaxing the stationary condition via an explicit grounding line migration. Omitting this (small) transitory term, the pivotal result is the existence of a relationship between ice flux and thickness at the grounding line (in agreement with Chugunov and Wilchinsky, 1996; Wilchinsky and Chugunov, 2001). The fundamental question of whether this problem has a unique solution remains open (Schoof and Hewitt, 2013). Numerical solutions suggest that the solution may not be unique, but rather span a narrow range (Nowicki and Wingham, 2008). The underlying reason concerns contact inequalities (absent in Chugunov and Wilchinsky, 1996) that must be met on either side of the contact line. Already suggested by Hindmarsh (1993), numerical results also support the hypothesis that ice discharge through the grounding line could be history dependent in the absence of sliding (Nowicki and Wingham, 2008), yet further analytical work is needed.

The case of rapid sliding is simpler, since a depth-integrated membrane model can be used for both floating and grounded regions (Schoof, 2007b). Asymptotic matching with a boundary layer near the grounding line yields a flux boundary condition for both depth-integrated (Schoof, 2007b) and full-Stokes (Schoof, 2011) models, under the assumption of continuous longitudinal stresses (across the grounding line). Numerically, the work of Nowicki and Wingham (2008) was also extended to the rapid sliding case by Durand and others (2009), showing good agreement with the asymptotic theory of Schoof (2007b).

Grounding lines present a situation where basal traction changes abruptly, yet this is also found in other regions such as the transition between frozen/thawed basal conditions (Hutter and Olunloyo, 1980; Barcilon and MacAyeal, 1993), glacier thrust faults (Kleman and Hättestrand, 1999; Moore and others, 2010), and deformable subglacial sediment beds (Schoof, 2004, 2012). The problem of the thermal bed transition of mountain glaciers was first investigated by Hutter and Olunloyo (1980) using a Wiener-Hopf method, concluding that the normal stresses are singular and concentrated at the transition. A more sophisticated version of the problem was then tackled by Barcilon and MacAyeal (1993), following the mathematical treatment presented in Richardson (1970). Barcilon and MacAyeal (1993) additionally consider a free surface that could ultimately reveal changes in basal conditions, motivated by the increasing satellite data. The authors estimate a surface deflection of $\sim 20\%$ ice thickness over the transition, though singularities in ice pressure exhibit an inconsistency with the necessary assumptions that justify a solution.

Abrupt changes in basal conditions are also present across the ice flow direction, particularly in the ice-stream shear margins (e.g., Raymond, 1996; Jackson and Kamb, 1997). While the central part of these fast flowing regions is dominated by longitudinal stresses, the behaviour in the side margins is rather complex, involving lateral shearing and thermoviscous feedbacks that potentially form temperate ice (Schoof, 2012; Meyer and Minchew, 2018). Idealised models for shear margins thus cope with an abrupt transition from free-slip to no-slip at the ice-bed interface (Perol and Rice, 2015; Meyer and others, 2016), where the development of temperate ice dictates its location, and it has been obtained both numerically (Jacobson and Raymond, 1998; Suckale and others, 2014) and analytically (Schoof, 2004, 2012). Under plastic bed conditions, Schoof (2004) showed that sliding zones across the ice flow are part of the solution and thermomechanically controlled by heat dissipation. Therefore, the extent of the sliding region cannot be arbitrarily prescribed, as simplistic assumptions produce stress singularities at the shear margins. The temperature solution allows to determine the speed of the transition point based on the obstacle problem constrains (Fowler, 2013), resembling the method used in studying grounding line dynamics (Nowicki and Wingham, 2008).

A fundamental caveat of idealised models investigating the frozen/thawed transition is the absence of sub-temperate sliding (Shreve, 1984; Fowler, 1986), first suggested by laboratory experiments illustrating that regelation occurs a few degrees below melting point (Telford and Turner, 1963; Gilpin, 1980). The assumption that a sliding law only applies when the basal temperature reaches the pressure melting point is incorrect (Fowler and Larson, 1978, 1980), and it leads to either velocity (Huybrechts and Payne, 1996)

or stress (Hutter and Olunloyo, 1980) discontinuities (singular in the latter). Instead, gradual subglacial water production should be considered through a continuous increase in sliding over a small temperature range as the melting point is approached (i.e., ~ 1 K, Fowler, 2011), and values implemented in models often range from -3.0 to -0.5°C (Pollard and DeConto, 2009, 2012; Pattyn, 2017). This captures the mechanism by which the ice starts to slide when pressure variations across the bedrock are sufficient to partially melt the ice, thus lubricating the base in patches (Robin, 1976; Hindmarsh and le Meur, 2001; Pattyn and others, 2004). The so-called patched lubrication suggests that sub-temperate sliding may occur in the transition between frozen (no-slip) to temperate beds (free-slip), supported by molecular adhesion (Raraty and Tabor, 1958; Barnes and others, 1971) and the predicted existence of isolated frozen parcels at the ice-bed interface of temperate glaciers (Robin, 1976).

The absence of sub-temperate sliding further leads to the paradox of a refreezing bed (Mantelli and others, 2019). If sliding is discontinuous (i.e., a "hard switch" transition), rapid vertical advection of cold ice associated with the horizontal speed-up inevitably refreezes the bed across the transition. A region of sub-temperate sliding thus alleviates the problem of rapid down-draw of cold ice, and yields a smooth transition between the two regimes. The stability of such a construction is investigated by Mantelli and Schoof (2019), concluding that steady-state solutions are unstable, hence leaving open the question of how the transition from a cold (non-sliding) to a temperate bed (sliding) operates.

Here, we analytically solve a long-standing problem in glaciology: the flow of a viscous ice stream across a no-slip to free-slip transition. The problem formulation parametrises the horizontal extent of the basal transition to study potential changes in flow behaviour. The velocity and pressure fields are smooth and well-behaved throughout the transition, overcoming previous difficulties. Exact solutions demonstrate that singularities in pressure are restricted to discontinuous bed transitions. The structure of the ice flow exhibits an overturning circulation, indicating that the stratigraphic sequence of the ice cores can be biased if collected downstream of the basal transition. A simple ice-sheet–shelf junction is constructed from the analytical solutions, and admissible grounding line positions are identified by exploring a range of ice flux values. Results show that the grounding line position is not univocally determined by the ice flux in the linearised problem, demonstrating that equilibrium positions are not discrete, but rather form a continuos set of solutions. This work sheds light on the physical behaviour of a complex mechanical region that fundamentally controls the Antarctic mass balance, while providing a benchmark framework to test ice-sheet models.

PROBLEM DEFINITION

We account for the simplest problem that embodies a change in the basal friction of an ice stream: the flow of a layer of viscous fluid overlying a boundary which changes from no-slip to stress-free (Fig. 1). The upper surface of the layer is assumed stress-free, and can adopt a shape consistent with the conditions at the base. The lower boundary parametrises the horizontal extent of the change from no-slip to free-slip conditions in the direction of the flow. This is the novelty of the formulation, aimed to circumvent the expected singularities in the flow over abrupt transitions (Batchelor, 1976; Richardson, 1970; Carrier, 2014). Robust physical motivation supports this choice, since the assumptions for a discontinuous sliding law are incorrect, and sub-temperate sliding naturally reflects the gradual production of a liquid water layer in polythermal conditions (Fowler and Larson, 1980; Fowler, 2011).

To ensure analytical tractability, the problem considers the steady-state Navier-Stokes flow of an incompressible, homogeneous and Newtonian fluid. The x-axis lies along the basal boundary and the z-axis is normal to the latter (Fig. 1). In this coordinate system, the steady Navier-Stokes equations read:

$$\begin{cases} \rho(uu_x + wu_z) & = -p_x + \mu\nabla^2 u + \rho g \sin\alpha \\ \rho(uw_x + ww_z) & = -p_z + \mu\nabla^2 w - \rho g \cos\alpha \\ u_x + w_z & = 0 \end{cases} \tag{1}$$

where $u(x,z)$ and $w(x,z)$ are the velocity components along the x and z axis, $p(x,z)$ is the pressure, ρ is the constant density, μ is the viscosity, g is the gravitational constant and α is the slope angle. Subscripts denote partial differentiation.

The left lateral boundary represents no-slip conditions via a parabolic profile (i.e., Poiseuille flow, Batchelor, 1976):

$$\left.\begin{aligned} u &= 3az\left(1 - \frac{z}{2}\right) \\ w &= 0 \end{aligned}\right\} \quad \text{at} \quad x = 0, \tag{2}$$

and the right boundary depicts a laminar flow in the absence of vertical shear, corresponding to free-slip conditions (plug flow):

$$\left.\begin{aligned} u &= a \\ w &= 0 \end{aligned}\right\} \quad \text{at} \quad x = L, \tag{3}$$

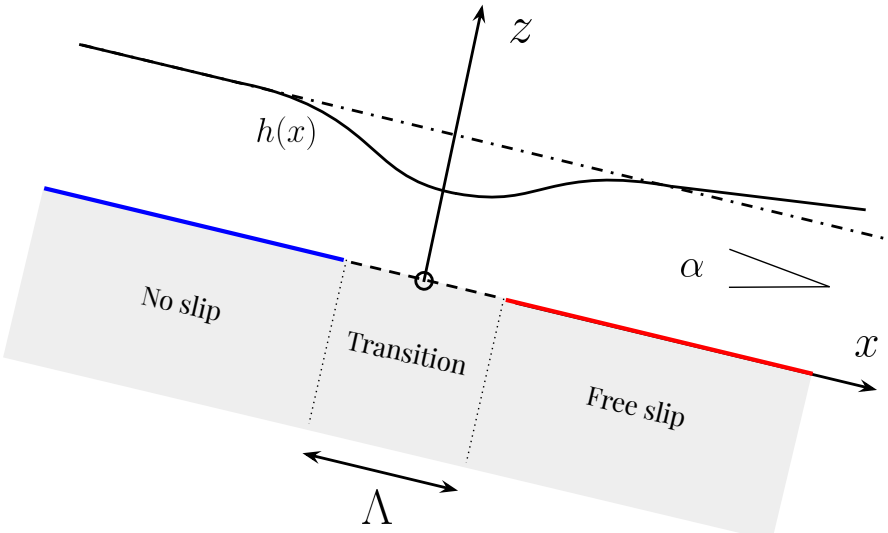

Fig. 1. Steady Navier-Stokes flow of a 2D viscous ice stream over an inclined plane. The basal transition from no-slip to free-slip leads to a regime shift from Poiseuille to plug flow. Note that the point-wise sharp transition is replaced by a smooth functional dependency of parametrised horizontal length Λ.

where the total flux $q = \int_0^h u dz$ is determined by the parameter a.

The basal boundary conditions are:

$$\left.\begin{aligned} u &= f(x,\Lambda) \\ w &= 0 \end{aligned}\right\} \quad \text{at} \quad z = 0 \tag{4}$$

where $f(x,\Lambda)$ is a functional dependency that characterizes the horizontal scale of the transition from no-slip to free-slip in terms of the parameter Λ. The values of $f(x,\Lambda)$ at the lateral boundaries are consistent with the Poiseuille and plug flow, respectively.

On the free surface $z = h(x)$, the stresses must be continuous. In other words, they must have values identical to those of air (assumed to be at rest). Setting the atmospheric pressure to zero at the surface interface for convenience, we find that:

$$\left.\begin{aligned} -h_x\left(-p + 2\mu u_x\right) + \mu\left(u_z + w_x\right) &= 0 \\ -h_x\mu\left(u_z + w_x\right) + \mu\left(-p + 2\mu w_z\right) &= 0 \end{aligned}\right\} \quad \text{at} \quad z = h(x), \tag{5}$$

ensuring that the surface is not subject to tangential stress.

The formulation is completed by imposing that there is no mass transfer between the atmosphere and the free surface of the ice:

$$w = uh_x \quad \text{for} \quad z = h(x). \tag{6}$$

This kinematic boundary condition ensures that the displacement along the z-axis follows the free surface curvature.

Small slope approximation

Despite these assumptions, the problem remains too complex for analytical treatment. If the slope α is considered small, a linearized version of the problem can be obtained through a perturbation analysis in α (a detailed derivation of the Taylor expansion can be found in Barcilon and MacAyeal, 1993).

The zeroth-order problem is trivial since it does not involve the flow: the ice surface is parallel to the bed everywhere $h^{(0)}(x) = H$ and the pressure is hydrostatic $p^{(0)}(z) = \rho g(H - z)$. The flow arises considering the first-order problem in α, where the Navier-Stokes equations (Eq. 1) can be written as:

$$\begin{cases} 0 &= -p_x^{(1)} + \mu\nabla^2 u^{(1)} + \rho g \\ 0 &= -p_z^{(1)} + \mu\nabla^2 w^{(1)} \\ 0 &= u_x^{(1)} + w_z^{(1)} \end{cases} \tag{7}$$

with the corresponding boundary conditions:

$$\left.\begin{aligned} -h^{(1)}p_z^{(0)} - p^{(1)}2\mu w_z^{(1)} &= 0 \\ u_z^{(1)} + w_x^{(1)} &= 0 \end{aligned}\right\} \quad \text{at} \quad z = h^{(0)}(x) \tag{8}$$

The kinematic boundary Eq. 6 condition is simplified to:

$$w^{(1)} = 0 \quad \text{for} \quad z = h^{(0)}(x). \tag{9}$$

Lastly, the bottom boundary condition translates to:

$$\left.\begin{aligned} u^{(1)} &= f(x,\Lambda) \\ w^{(1)} &= 0 \end{aligned}\right\} \quad \text{at} \quad z=0 \tag{10}$$

where $f(x,\Lambda)$ is a sigmoid function that characterizes the horizontal extent of the transition from no-slip to free-slip:

$$f(x,\Lambda) = \frac{a}{1+e^{-\frac{1}{\Lambda}(x-L/2)}}, \tag{11}$$

where the numerator a is imposed for consistency with the lateral boundary conditions.

The parameter Λ determines the horizontal length scale over which the sigmoid responds, yielding sharper transitions as Λ decreases. The transition is thus equivalent to Barcilon and MacAyeal (1993) in the limit $\Lambda \to 0$ (i.e., where the transition becomes discontinuous).

The lateral boundary conditions maintain the same structure as in the full problem (Eq. 2 and 3), but explicitly referred to the first-order flow response $u^{(1)}$ and $w^{(1)}$.

ANALYTICAL SOLUTION

The physical problem (Fig. 1) translates mathematically into solving the biharmonic equation in a finite 2D domain with the corresponding boundary conditions (Fig. 2). Introducing the dimensionless variables:

$$\tilde{x} = \frac{x}{H}, \quad \tilde{z} = \frac{z}{H}, \quad \tilde{u} = \frac{\rho g H^2}{\mu} u^{(1)}, \quad \tilde{w} = \frac{\rho g H^2}{\mu} w^{(1)}, \quad \tilde{p} = \frac{p^{(1)}}{\rho g H}, \quad \tilde{h} = \frac{h^{(1)}}{H}, \tag{12}$$

where tildes are hereinafter dropped to lighten the notation.

The first-order problem takes the following succinct form:

$$\begin{cases} 0 &= -p_x + \nabla^2 u + 1 \\ 0 &= -p_z + \nabla^2 w \\ 0 &= u_x + w_z \end{cases} \tag{13}$$

with the corresponding boundary conditions:

$$w = u_z = 0 \quad \text{at} \quad z = 1, \tag{14}$$

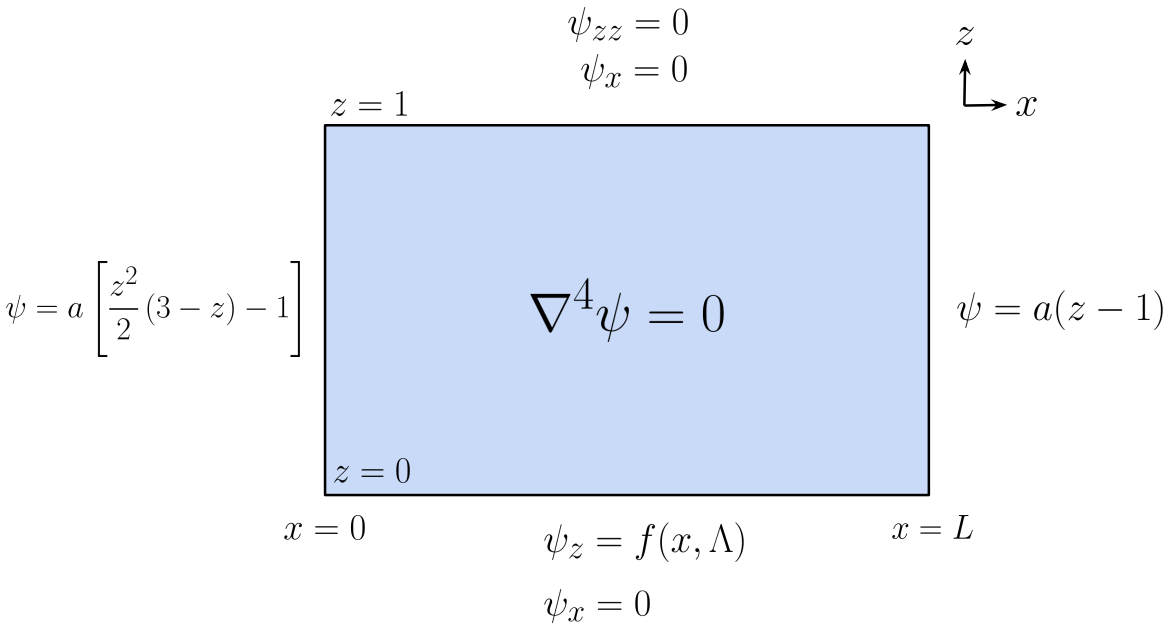

Fig. 2. Mathematical formulation of the problem. The imposed lateral boundary conditions correspond to Poiseuille flow ($x = 0$) and plug flow ($x = L$). The steady Navier-Stokes flow of a 2D viscous glacier is mathematically equivalent to solving the biharmonic equation $\nabla^4\psi = 0$. The basal boundary condition $f(x, \Lambda)$ captures a transition from no-slip to free-slip consistent with Poiseuille and plug flow, respectively.

and:

$$\left.\begin{aligned} u &= f(x, \Lambda) \\ w &= 0 \end{aligned}\right\} \quad \text{at} \quad z = 0. \tag{15}$$

The deflection of the upper surface can be computed from the dynamical boundary condition Eq. 8 once the problem is solved (Eq. 13):

$$h = p - 2w_z \quad \text{at} \quad z = 0. \tag{16}$$

We shall introduce the stream function $\psi(x, z)$, where the velocity components are defined as:

$$\begin{cases} u &= \psi_z \\ w &= -\psi_x. \end{cases} \tag{17}$$

so that the problem reduces to solving the biharmonic equation $\nabla^4\psi = 0$ (Batchelor, 1976).

Separation of variables

The finite domain definition allows the problem to be solved by separation of variables (also known as the Fourier method), rather than dealing with a Wiener-Hopf equation as in previous studies (e.g., Richardson, 1970; Hutter and Olunloyo, 1980; Barcilon and MacAyeal, 1993). This technique has previously been used in glaciology to obtain exact transitory solutions of ice temperatures (Moreno-Parada and others, 2024). The horizontal extent of the domain is chosen so that the lateral boundary conditions do not interfere with the solution near the basal transition.

The separation of variables requires both the problem and the boundary conditions to be linear, thus ensuring the superposition of all normal modes. The problem has inhomogeneous boundary conditions (as formulated in Fig. 2), and a change of variables is needed to obtain homogeneous boundary conditions and compute the eigenvalues. Given the polynomial form of the lateral boundary conditions in the x-axis (Fig. 2), a simple transformation:

$$\tilde{\psi}(x,z) = \psi(x,z) - \psi(0,z)\left(1 - \frac{x}{L}\right) - \psi(L,z)\left(\frac{x}{L}\right), \tag{18}$$

yields homogeneous boundary conditions along the x-axis, permitting the expansion in eigenfunctions in such direction (see Appendix for derivation details). In the vertical axis, orthogonality of the eigenfunction ensures that boundary conditions are met: basal transition and the free-stress upper surface.

The standard separation of variables approach looks for solutions of the form:

$$\tilde{\psi}(x,z) = X(x)Z(z), \tag{19}$$

where the functions $X(x)$ and $Z(z)$ are to be determined. Using the ansatz in Eq. 19, it follows:

$$\frac{X_{xxxx}}{X} + 2\frac{X_{xx}Z_{zz}}{XZ} + \frac{Z_{zzzz}}{Z} = 0, \tag{20}$$

Upon differentiation with respect to z, we can obtain a separable equation:

$$\frac{X_{xx}}{X} = -\frac{1}{2}\frac{Z_{zzzzz}Z - Z_{zzzz}Z_z}{Z_{zzz}Z - Z_{zz}Z_z} = +\lambda^2, \tag{21}$$

for some constant λ.

The solution $\tilde{\psi}(x,z) = X(x)Z(z)$ of the first-order Navier-Stokes problem must satisfy these equations. The problem has been reduced to solving two ODEs. For the z-axis, the fourth-order ODE reads:

$$Z_{zzzz} - 2\lambda^2 Z_{zz} + \lambda^4 Z = 0, \tag{22}$$

yielding a solution of the form $Z(z) = (A + Bz)\, e^{\lambda z} + (C + Dz)\, e^{-\lambda z}$.

Analogously, we find a second-order ODE along the x-axis:

$$X_{xx} - \lambda^2 X = 0, \tag{23}$$

where direct integration results in $X(x) = E\, \cos(\lambda x) + F\, \sin(\lambda x)$.

Given that the problem and the boundary conditions are linear, any linear combination of a sequence of solutions is also a solution. Under proper convergence assumptions, an infinite series will also be a solution. After imposing boundary conditions over the x-axis (i.e., $E = 0$), the general solution reads:

$$\tilde{\psi}(x,z) = \sum_{n=0}^{\infty} \sin(\lambda_n x) \left[(A_n + B_n z)\, e^{\lambda_n z} + (C_n + D_n z)\, e^{-\lambda_n z} \right], \tag{24}$$

where $\lambda_n = n\pi/L$, and the coefficients A_n, B_n, C_n and D_n are determined from the boundary conditions imposed on the z-axis (see Appendix for derivation details).

The problem is now analytically solved: velocities and pressure can be obtained upon differentiation directly from the stream function (Eq. 24), while the surface deflection is readily computed by the boundary condition (Eq. 16). Different horizontal scales of the basal transition are considered, as parametrised by Λ. The results are first presented for $\Lambda = 0.1$, where Λ has the same units as x (Eq. 11). Since the coordinate system is normalised by the unperturbed ice thickness H, a value $\Lambda = 0.1$ implies that the transition from no-slip to free-slip has a natural length of $0.1 \cdot H$ (i.e., a 10% of the unperturbed thickness).

The velocity fields are smooth and consistent with the imposed boundary conditions (Fig. 3). For the horizontal component of the velocity, a parabolic profile at $x = 0$ and plug flow $x = L$ are found at the lateral boundaries. At the base ($z = 0$), the velocity remains strictly zero until the transition is approached, resulting in a gradual increase within the horizontal scale dictated by Λ, and centred in the midpoint $x = L/2$. The velocity magnitude remains constant along the x-axis. The vertical component of the velocity is symmetric with respect to the axis of the transition location ($x = L/2$), reaching a global

minimum in the lower half.

The structure of this subsidence entails a pressure drop at $x = L/2$, reaching negative values due to the vertical velocity gradients along the z-axis (Fig. 3c). The vertical extent of the pressure drop is limited to the lower $\sim 20\%$ of the ice thickness. Upstream of the transition, the pressure shows a slight increase that leads to an upper surface elevation (Fig 4c). As the transition is approached, the vertical gradients in w overcome the increase in pressure, and yield surface deflection. The free surface exhibits a minimum that is found upstream of the symmetry axis of the basal transition. Downstream, the gradients w_z decrease, the pressure shows a linear increase, and so does the free surface.

HORIZONTAL SCALE OF THE BASAL TRANSITION

The introduced parameter Λ simply controls the horizontal scale of the basal transition from no-slip to free-slip via a smooth sigmoid function (Eq. 11). This permits to study the solution behaviour in terms of Λ, while avoiding the singular behaviour expected for abrupt boundary conditions.

Sufficiently large values of Λ entail positive values of both pressure $p(x, z)$ and vorticity $\eta(x, z) = u_z - w_x$ (Fig. 5). As the transition becomes sharper, the basal pressure narrows and deepens around the transition ($x = L/2$), reflecting a localised response in the flow (Fig. 5 and Fig. 4d). As a result, the free surface elevation only shows deflection if the basal transition is sharp. These results align with previous numerical work in similar setups, where surface deflection across the ice-sheet–ice-shelf transition is only found where grounded ice is not allowed to slide (Nowicki and Wingham, 2008). Minor differences are only found regarding the location of the surface local minimum: our analytical solution reaches the lowest value upstream of the transition, as opposed to the downstream minimum in the numerical results of Nowicki and Wingham (2008).

The vorticity also exhibits a regime shift as Λ decreases (Fig. 5a and 5b). Negative values are reached, illustrating that an overturning in the ice flow is possible downstream of the transition. The vorticity structure around the transition is mainly dictated by the vertical velocity therein, given the large horizontal gradients in w compared to the vertical gradients in u (Fig. 3).

The discontinuous transition limit

As already noted by Barcilon and MacAyeal (1993), difficulties related to singularities in pressure arise if the transition is discontinuous (i.e., the sliding regime initiates at a given piecewise location). In terms of

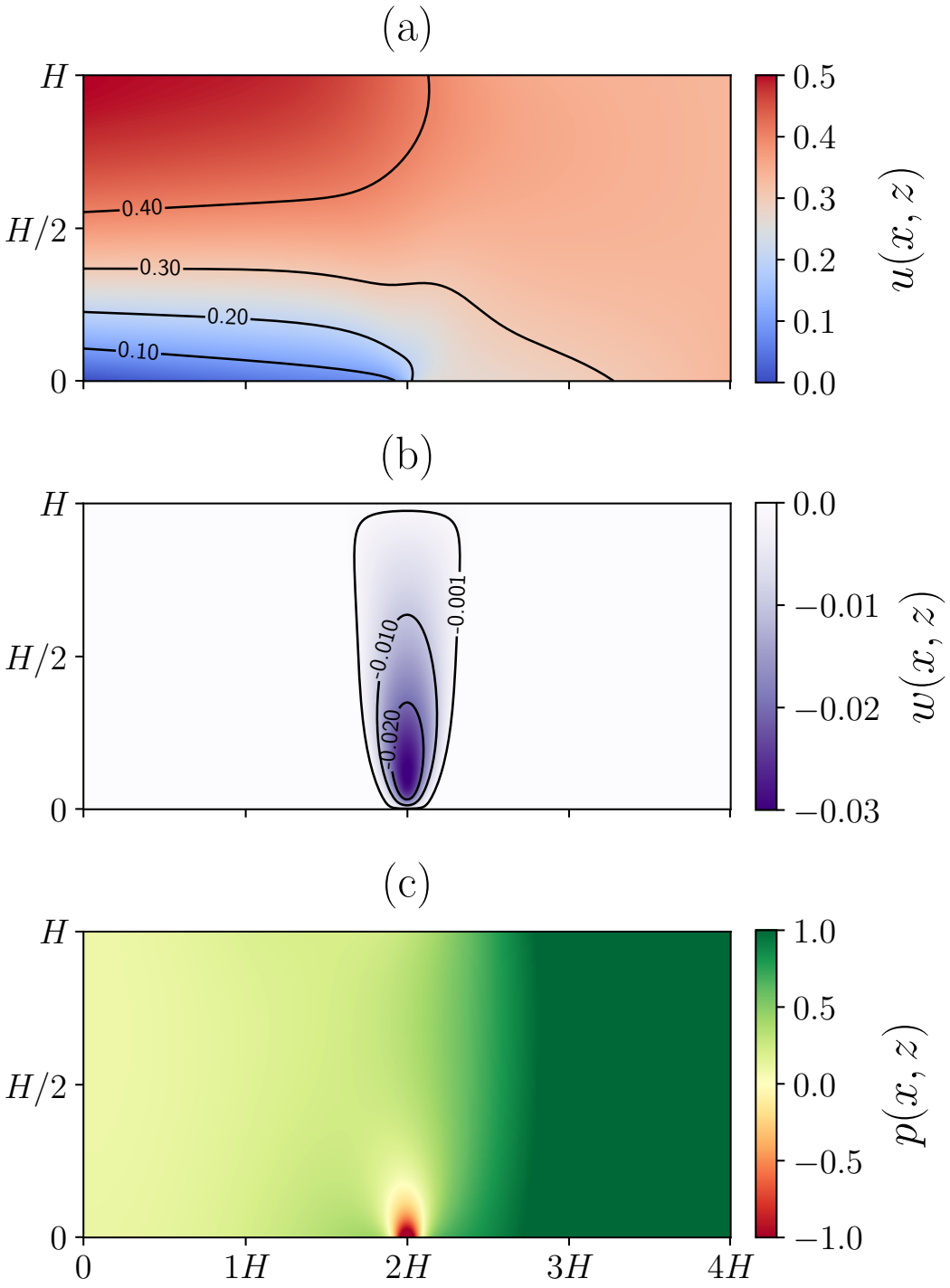

Fig. 3. Velocity and pressure solutions from Eq. 24: (a) Horizontal component $u(x, z)$, (b) Vertical component $w(x, z)$, and (c) Pressure field $p(x, z)$. Poiseuille and plug flow are imposed as lateral boundary conditions at $x = 0$ and $x = L$, respectively. In all panels, $\Lambda = 0.05$.

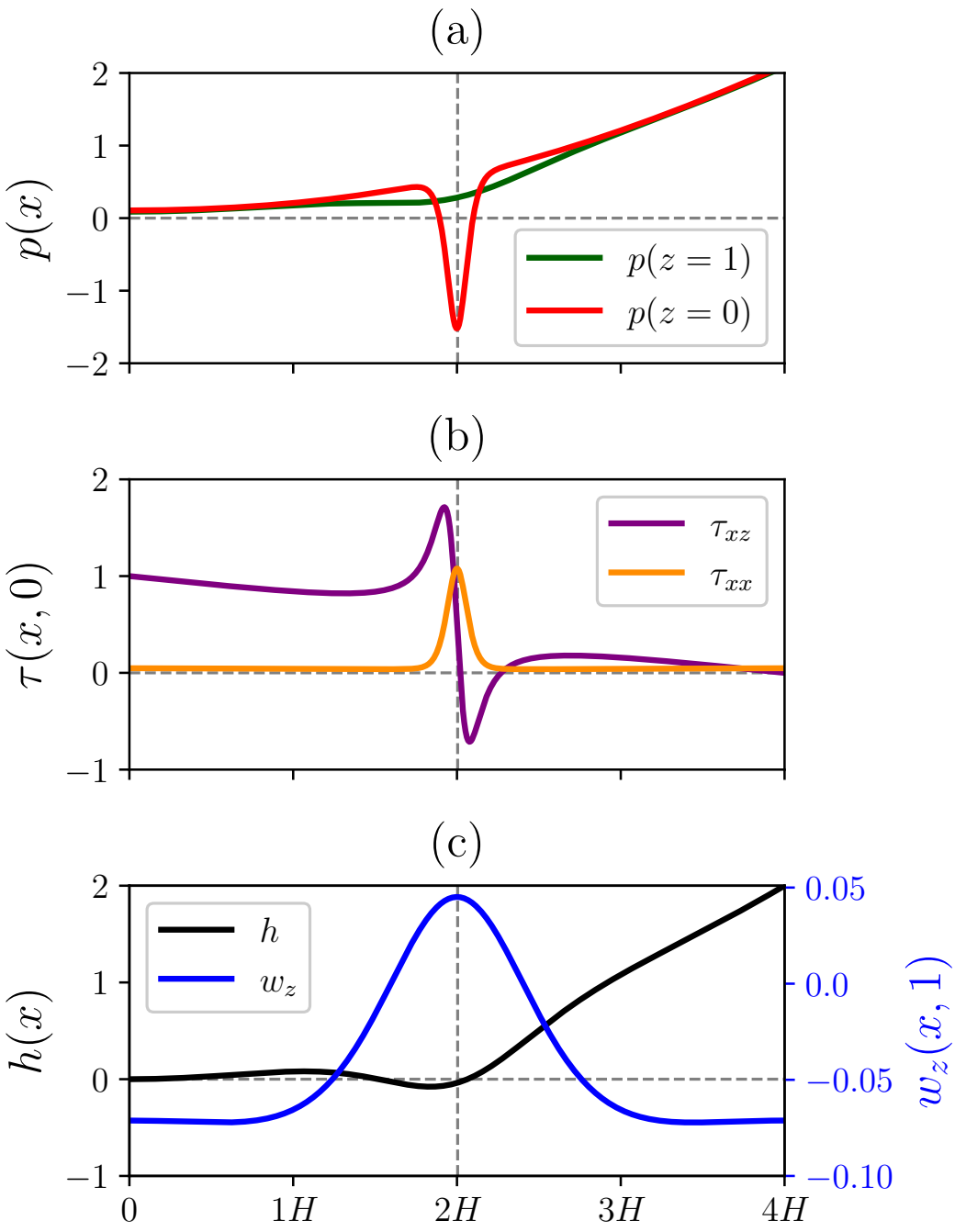

Fig. 4. (a) Pressure solutions. (b) Stresses. (c) Free surface elevation (black) and vertical velocity gradient (blue) along the z-axis. Note that the linear increase in the free surface is compensated by the downwards sloping bed (i.e., the zeroth-order surface incline), yielding the total height $h^{(0)} + \alpha h^{(1)}$ horizontal. $\Lambda = 0.05$ in all panels.

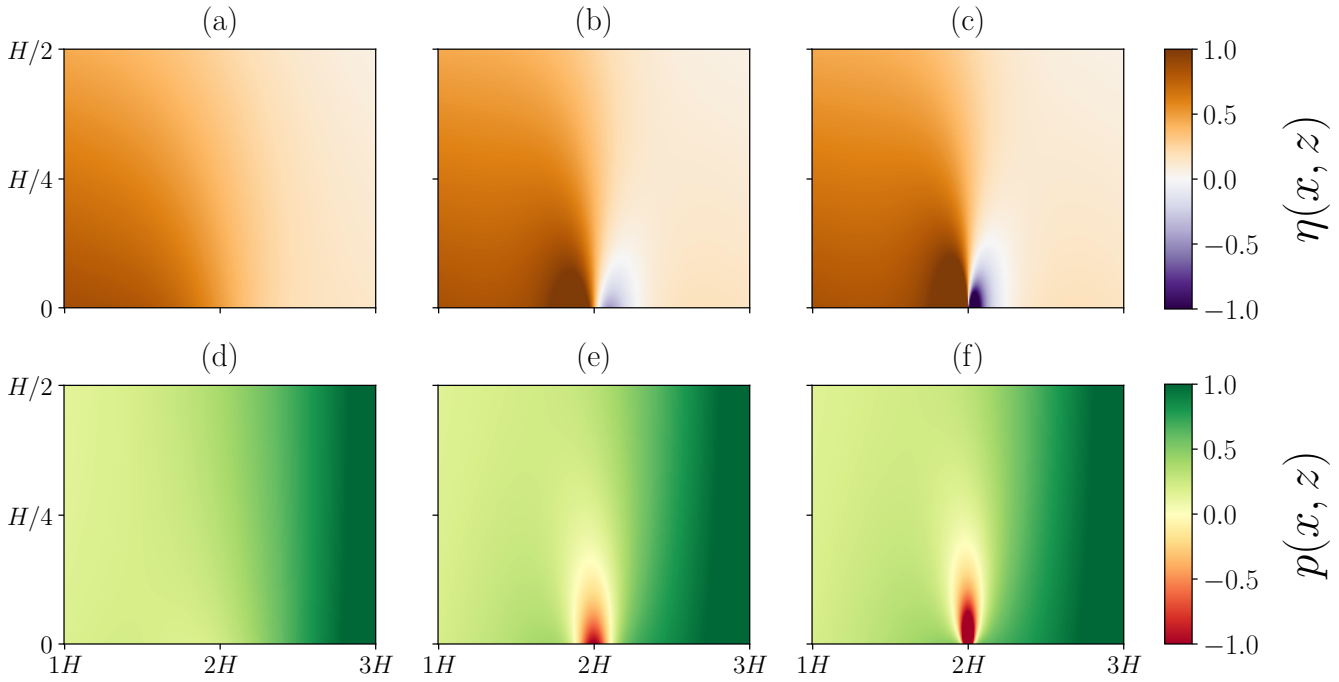

Fig. 5. Vorticity $\eta(x, z)$ (first row) and pressure field $p(x, z)$ (second row) for $\Lambda = 0.25$ (first column), $\Lambda = 0.05$ (second column), and $\Lambda = 0.01$ (third column). Note that that both spatial axes are zoomed in onto the basal transition.

our formulation, this scenario is equivalent to $\Lambda \to 0$, where the transition exhibits a step behaviour.

This section shows that the pressure singularity appears precisely in the limit $\Lambda \to 0$, demonstrating that it is purely the result of an idealised domain formulation (as singularities are typical of abrupt changes in boundary conditions, England and Sih, 1971). To prove it, we denote by ζ the harmonic conjugate of vorticity η, so that both functions satisfy the Cauchy-Riemann conditions $\eta_x = \zeta_z$ and $\eta_z = -\zeta_x$. This permits to express the momentum balance (Eq. 13) as:

$$\begin{cases} 0 &= -p_x - \zeta_x + 1 \\ 0 &= -p_z - \zeta_z \end{cases} \tag{25}$$

Direct integration allows to compute the pressure:

$$p(x, z) = x - \zeta(x, z) + C, \tag{26}$$

where C is a constant.

The problem now reduces to understanding the convergence behaviour of $\zeta(x, z)$. From our solution

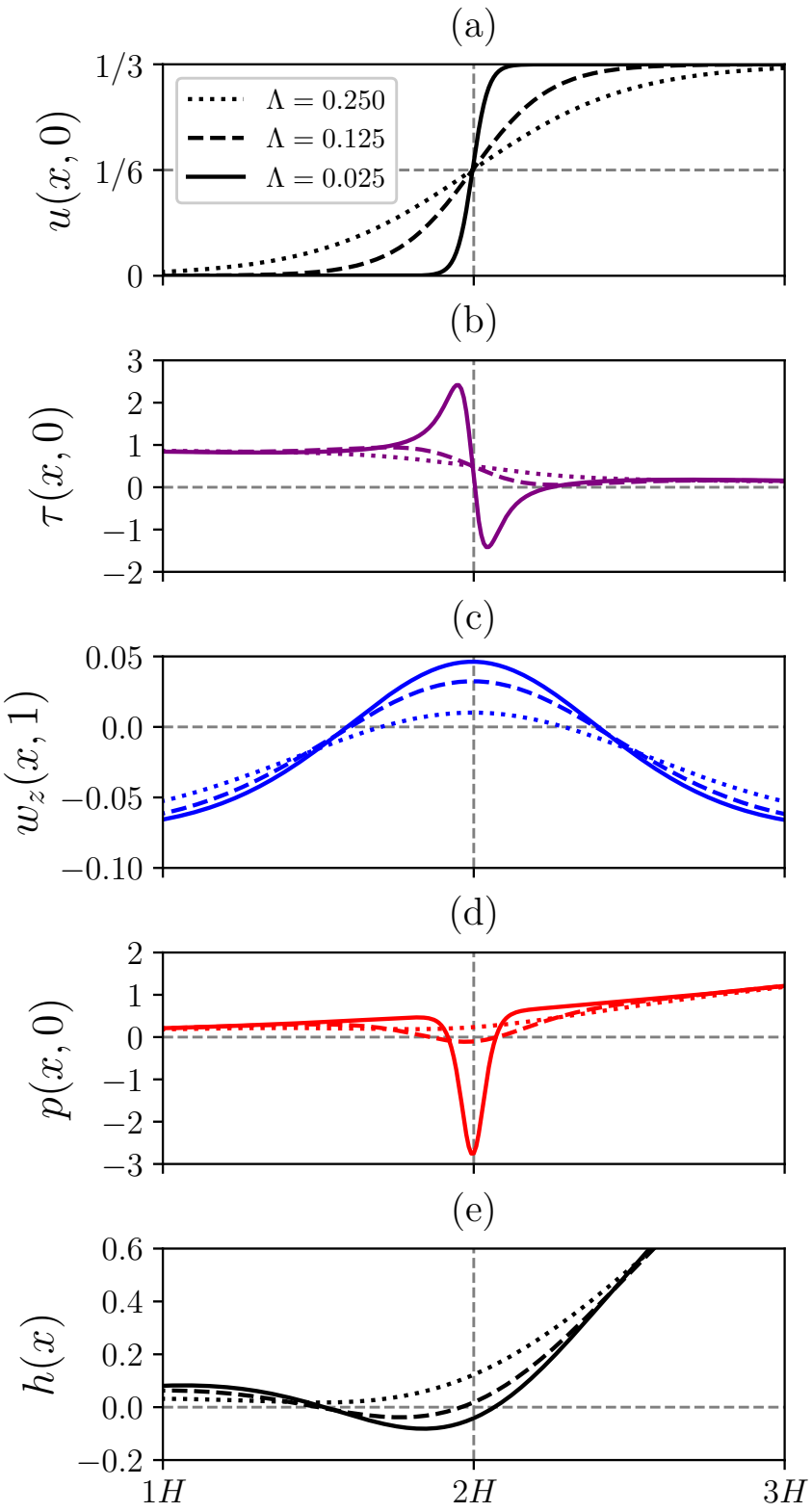

Fig. 6. Sensitivity to basal transition length scale Λ. (a) Basal boundary condition $u(x,0)$. (b) Vertical shear stress $\tau = u_z(x,0)$. (c) Surface vertical velocity gradient along the z-axis $w_z(x,1)$. (d) Basal pressure $p(x,0)$. (e) Free surface elevation $h(x)$ (first-order perturbation). Note that the x-axis spans $\pm 1H$ around the transition.

(Eq. 24), we can directly obtain the corresponding value centred at the transition ($x = L/2, z = 0$):

$$\zeta(L/2,0) = \sum_{n=1}^{\infty} 2\lambda_n \cos\left(\frac{n\pi}{2}\right)\left[-2\lambda_n A_n - 2C_n + D_n\right]. \tag{27}$$

Since the coefficients are obtained analytically, direct inspection shows an exponential decay in all coefficients, but D_n (see Appendix). The only non-vanishing term yields:

$$\zeta(L/2,0) \sim \sum_{n=0}^{\infty} \lambda_n \cos\left(\frac{n\pi}{2}\right) F_n. \tag{28}$$

We first consider the smooth and continuous transition. For non-zero Λ, the sigmoid derivative is bounded by a positive constant, and there are no singularities in pressure given the symmetry of the expression for F_n (integrating by parts, see Appendix):

$$\zeta(L/2,0) \lesssim \sum_{n=1}^{\infty} \frac{\sin(n\pi)}{n} \cos\left(\frac{n\pi}{2}\right) = 0. \tag{29}$$

On the contrary, in the discontinuous case ($\Lambda \to 0$), the sigmoid function is equivalent to a step function (i.e., a Heaviside function centred at $x = L/2$), and the analytical integration of F_n exhibits $\mathcal{O}(1/n)$ convergence that is compensated by λ_n:

$$\zeta(L/2,0) \sim \sum_{n=1}^{\infty} \cos^2\left(\frac{n\pi}{2}\right) = \infty, \tag{30}$$

which clearly diverges.

This result demonstrates that the pressure at the transition only diverges if the basal transition is discontinuous, in agreement with previous analytical (Barcilon and MacAyeal, 1993) and numerical work (Lestringant, 1994; Chugunov and Wilchinsky, 1996; Nowicki and Wingham, 2008).

A SIMPLE ICE-SHEET–SHELF JUNCTION

The transition considered here simply reflects a change in basal friction (Eq. 4). This regime shift is found in a wide variety of domains, such as frozen/thawed conditions and deformable sediment beds. One of the most significant scenarios is the grounding zone, where shearing ice flows towards a frictionless inviscid ocean water. Although such a problem exhibits certain differences compared to our original formulation

(Eq. 7), it deserves attention given the geometrical simplicity.

The grounding line position is a free boundary problem; either implicitly time-dependent, as in Schoof (2007a), or explicit Stefan-type, as in Robison and others (2010), which requires further conditions to determine its position x_{gl}. These conditions are known as contact inequalities, and require (1) the lower boundary of the ice shelf to detach from the bed, and (2) the normal stress to attain or exceed the pressure that sea water would exert at such location (i.e., otherwise water would intrude between the ice and the bed). Denoting by $l = l(x)$ the height of the bottom surface of the ice shelf, the contact inequalities can be expressed as (Nowicki and Wingham, 2008):

$$\left.\begin{aligned} \boldsymbol{\sigma}\cdot\hat{\mathbf{n}} \geqslant -p_{\mathrm{w}}\hat{\mathbf{n}}, \qquad & z = b(x),\ x < x_{\mathrm{gl}} \\ l(x) > b(x), \qquad & z = l(x),\ x > x_{\mathrm{gl}} \end{aligned}\right\} \tag{31}$$

where p_{w} is the water pressure, $\hat{\mathbf{n}}$ is the unit normal vector to the boundary and $\sigma_{ij} = -p\delta_{ij} + \tau_{ij}$ is the Cauchy stress tensor in the normal and deviatoric decomposition (index notation).

It is illustrative to study the geometry of the ice sheet–shelf junction by including the corresponding boundary condition at the bottom of the ice shelf (assumptions in the problem formulation are described in the Discussion section). Downstream of the grounding line, the lower free surface corresponds to the ice-water interface of the ice shelf, and is obtained assuming inviscid conditions between the two fluids. The dimensionless dynamic condition therein reads (Schoof, 2011):

$$\left.\begin{aligned} (p + \varrho l - 2u_x)l_x + u_z + w_x = 0 \\ p + \varrho l + 2u_x + (u_z + w_x)l_x = 0 \end{aligned}\right\} \quad \text{at} \quad z = 0,\ x > x_{\mathrm{gl}}, \tag{32}$$

where $\varrho = \rho_w/\rho$ is the water-ice density ratio.

Given that the full Stokes problem is already solved (Eq. 24), we can readily obtain the shelf geometry $l = l(x)$ and study its behaviour for different fluxes and basal transitions (Fig. 7). Since we do not solve for a free boundary problem, the position of the grounding line is imposed before solving the Stokes problem (as in Nowicki and Wingham, 2008). This approach allows us to diagnose whether the imposed grounding line position satisfies the contact inequalities.

For simplicity, the position of the grounding line is set first at $x_{\mathrm{gl}} = L/2$ (Fig 7a). Upstream of x_{gl}, the upper surface is nearly parallel to the bed, as dictated by the zero-th order contribution $h^{(0)}$ (recall Fig 4c). Within the first half ice-thickness downstream of x_{gl} (from $x = 2.0$ to $x = 2.5$), the surface deflection

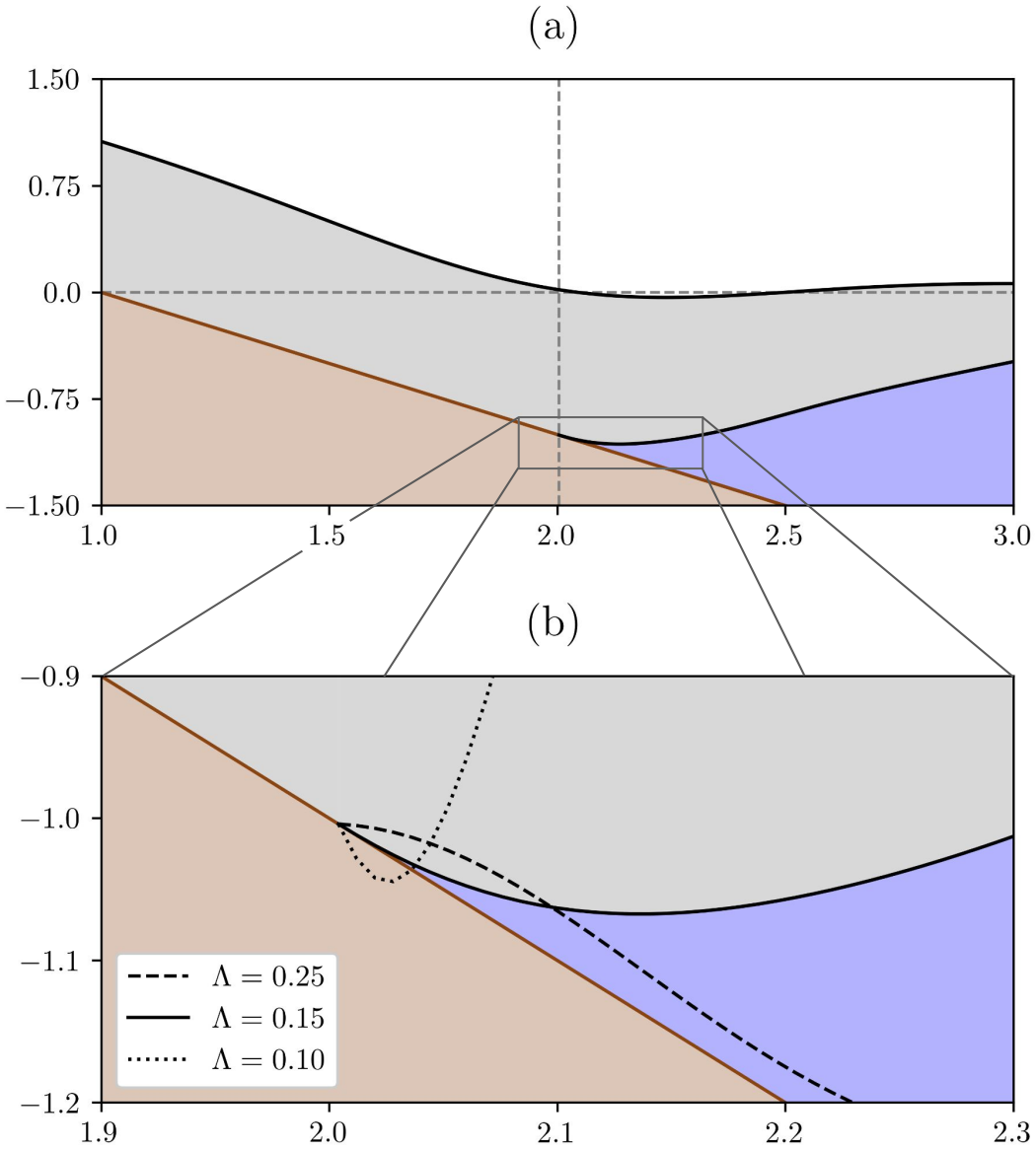

Fig. 7. Analytical free surfaces calculated from dynamic boundary conditions at the ice-air (upper surface) and ice-water (ice shelf bottom surface) interfaces, respectively. The grounded line position is imposed at $x_{\mathrm{gl}} = L/2$. (a) Ice-sheet–shelf transition. (b) Zoomed in region comparing three different transition regimes in terms of Λ. Note that $\Lambda = 0.10$ illustrates a Stokes solution violating the first contact inequality (i.e., the ice does not detach from the bedrock). The bedrock height is referred to the dimensionless small-slope approximation $\rho g \sin\alpha = 1$.

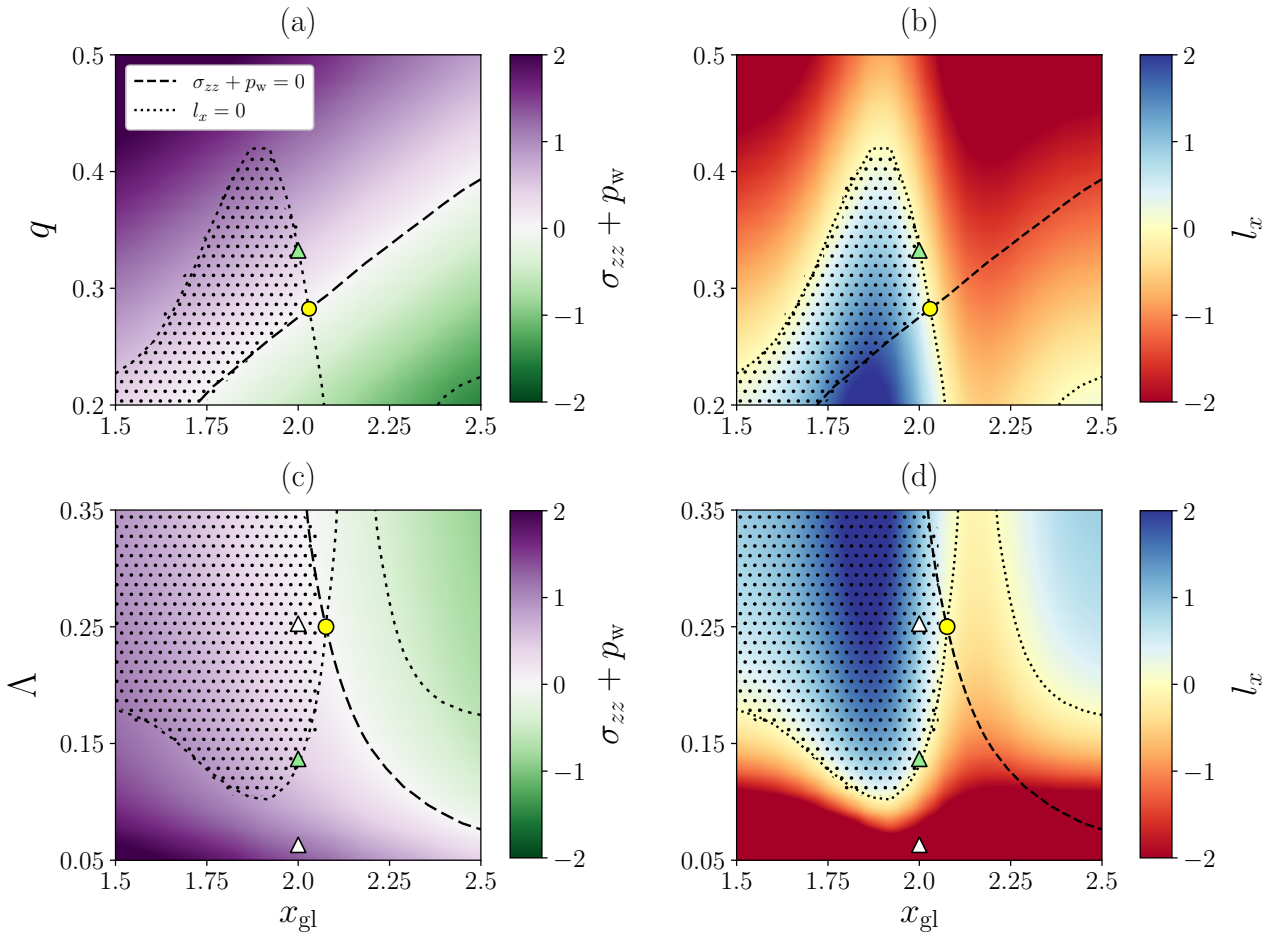

Fig. 8. Contact inequalities. Panels (a) and (c): total balance of ice normal stress σ_{zz} and water pressure p_w ($\Lambda = 0.25$). Panels (b) and (d): ice shelf lower boundary slope $l_x(x)$ ($q = 1/3$). The hatched dotted region represents pair values that satisfy both contact inequalities. The coloured triangles correspond to the solutions depicted in Fig. 7 (green, Fig. 7a; white, 7b). Yellow dots represent the limit solutions where the ice shelf detaches parallel to the bed ($l_x = 0$) and the ice normal stress equates the corresponding water pressure ($\sigma_{zz} + p_w = 0$).

reaches a minimum, beyond which the free surface becomes asymptotically flat. The lower boundary of the shelf detaches nearly paralell from the bed, and its shape sensitivity due to the basal transition is further shown in Fig 7b. Three different values are represented to illustrate the restriction of the second contact inequality (Eq. 31_2), only satisfied by the two highest values ($\Lambda = 0.15$ and 0.25), since the bottom of the ice shelf lies above the corresponding bedrock height. In contrast, $\Lambda = 0.10$ showcases a non-detaching shelf that is not permissible for the imposed grounding line position at $x_{gl} = L/2$, as the abrupt basal transition produces stress gradients capable of bending downwards the flow of ice (e.g., Ribe, 2001; Schoof, 2011).

A detaching ice shelf only meets one inequality for an admissible grounding line position, given that normal stresses must also attain the corresponding water pressure (Eq. 31). We next explore what values

of Λ and q simultaneously satisfy both contact inequalities for a fixed grounding line position (Fig. 8). From the pressure balance (Fig. 8a and 8c) and the bottom shelf geometry (Fig. 8b and 8d), it is possible to identify a region with admissible grounding line positions (black dotted hatch, Fig. 8). In other words, those flow solutions with an imposed grounding line satisfying both contact inequalities. Multiple values of Λ and q are admissible for a given location x_{gl}, implying that equilibrium positions are not discrete, but rather form a continuos set of solutions. An infinite number of pair values (Λ, q) within a certain range are compatible with a given grounding line position. As a result, the ice flux does not univocally determine the position of the grounding line under a small-slope approximation.

ASYMPTOTIC CONSISTENCY OF THE FIRST-ORDER PROBLEM

The linearized version of the problem was obtained by truncating a Taylor expansion in terms of the slope angle α. The pressure field then reads $p(x, z; \alpha) = p^{(0)} + \alpha p^{(1)} + \mathcal{O}(\alpha^2)$. This implies a uniform ordering assumption in the series, meaning that the zeroth-order pressure $p^{(0)}$ must remain larger than the first-order perturbation $p^{(1)}$. In other words, the expansion must be asymptotically consistent everywhere in the fluid. This can be expressed in terms of dimensionless variables as:

$$\max_{x,z} \ |\alpha p^{(1)}| \ll 1, \tag{33}$$

Violating this condition only means that the linearization fails locally, not that the solution is unphysical. Hence, the validity of the linear approximation can be determined in terms of α for different values of q and Λ (Fig. 9). As pressure singularities are prone to arise at the basal transition, Eq. 33 is evaluated at $x = L/2$. Since the solution is expressed as an Fourier infinite series, truncation is performed at order $n = 10^3$ (Eq. 24).

The results show that the linear problem in α (Eq. 7) yields asymptotically consistent solutions in the parameter range explored in this study for reasonable bed slopes $\alpha = 10^{-4} - 10^{-2}$ (Fig. 9). In particular, grounding line solutions that produce vanishing (first-order) pressures at $x = x_{\mathrm{gl}}$ are asymptomatically consistent for any slope angle. The physical reason is that the parameter values compatible with such a solution cancel the downwards increase in pressure with the subsidence due to the basal drag transition (Fig. 6d). These solutions also correspond to admissible grounding line positions, as they satisfy both contact inequalities (green triangle, Fig. 8).

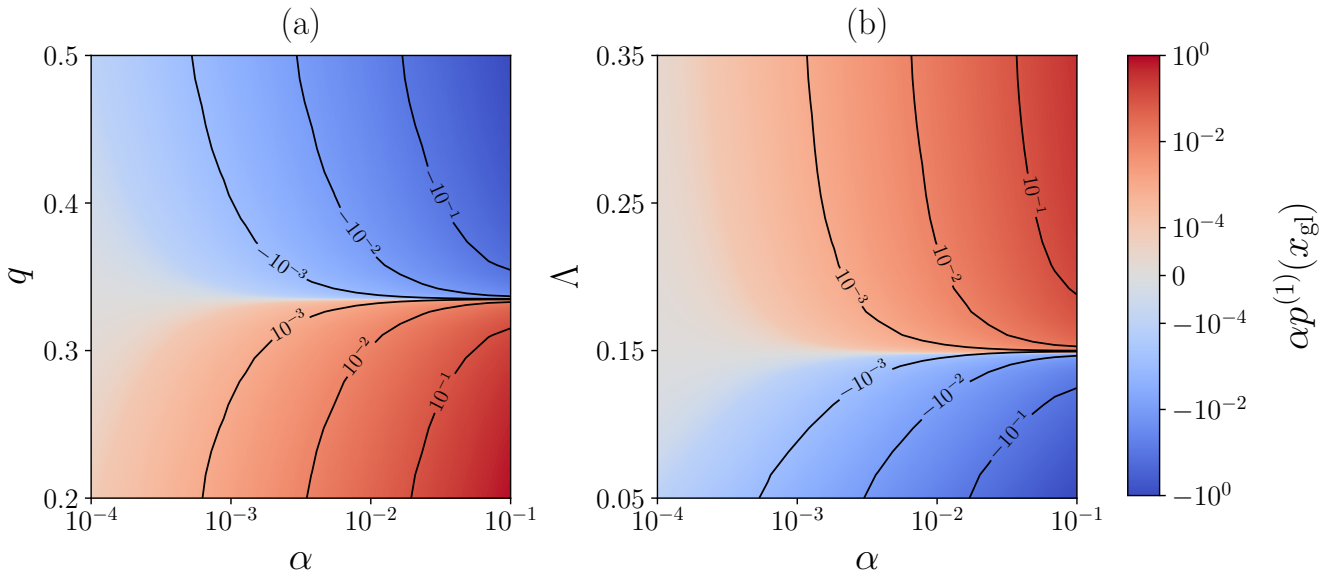

Fig. 9. Asymptotic consistency of the first-order pressure solution $p^{(1)}$ evaluated at the imposed grounding line position $x_{gl} = L/2$ for different bed slopes α. (a) Dependency on the total ice flux q. (b) Dependency on the horizontal scale of the basal transition Λ. Note that the colour bar employs a symmetric logarithmic normalization with a linear region around $\pm 10^{-4}$.

DISCUSSION

Previous analytical and numerical work has aimed to understand the ice flow behaviour across a sharp basal friction transition. Ultimately, this is an idealised representation of a grounding zone (i.e., the creeping flow of ice transitions to rapid streaming over a frictionless ice shelve) or a frozen/thawed bed transition (e.g., polythermal bed conditions along the flowline direction in a glacier). Our analytical results align in several major points with prior studies. Both the overall structure of the ice flow and the existence of a free surface deflection agree with Barcilon and MacAyeal (1993), who first showed that the velocity solution across a discontinuous transition is smooth (rather than exhibiting a jump centred at the transition, Hutter and Olunloyo, 1980). Additionally, our exact solutions confirm the existence of a free surface deflection previously found in modelling results (Lestringant, 1994; Chugunov and Wilchinsky, 1996; Nowicki and Wingham, 2008; Durand and others, 2009).

The main novelty in the present study lies on the continuous and parametrised change of basal friction, strongly motivated by sub-temperate sliding. The predicted existence of patches of frozen ice ($\sim$ 0.1–1.0 metres wide, Robin, 1976) in temperate glaciers agrees with previous observations by Kamb (1970). This supports the idea that ice will start to slide if pressure variations across the bedrock are sufficient to melt isolated parcels, captured by a temperature-dependent sliding law near the melting point (Fowler and

Larson, 1978; Shreve, 1984; Fowler, 2011). Already motivated by early laboratory experiments (Raraty and Tabor, 1958; Barnes and others, 1971), this hypothesis suggests that molecular adhesion is present when glaciers slide at relatively low velocities (Robin, 1976). The so-called patched lubrication implies that sub-temperate sliding may occur in the transition between frozen (no-slip) to temperate beds (free-slip). This mechanism thus complements the usual assumption that a thin layer of liquid water separates the bedrock from the basal ice, fundamental in sliding theories of cavitation (Lliboutry, 1964, 1968).

Besides the robust agreement with previous work, the analytical results in this study provide deeper insight on the ice flow about the transition. We have mathematically proven that pressure solutions are finite and well-behaved, provided that the basal transition is continuous. This overcomes prior inconsistencies found in Barcilon and MacAyeal (1993), where the pressure becomes negatively infinite immediately downstream of the basal transition. Based on physical considerations, the authors pointed to additional processes to compensate for the infinite pressure (e.g., ice rheology and thermodynamics). Our results have shown that the singularity in pressure is purely a consequence of a discontinuous basal boundary condition. An idealised point-wise transition is mathematically sound, yet it modifies the flow structure. Instead, a continuous transition is sufficient to ensure a finite pressure field and the asymptotic consistency of the solution.

The other fundamental change in the ice flow structure concerns overturning circulation. Previous studies dismissed the possibility of such a behaviour on the basis of the ice vorticity properties (Barcilon and MacAyeal, 1993). However, this conclusion relies on the assumption that pressure is singular near the transition, which has been shown to be valid only on idealised discontinuous transitions. Analytical solutions exhibit sign changes in vorticity across the transition, demonstrating that small eddies of recirculating flow are possible. Unlike previously stated (Barcilon and MacAyeal, 1993), the stratigraphic sequence of ice cores collected downstream can be overturned by the no-slip to free-sleep transition in the bed (as first shown by Weertman, 1976).

Previous studies aiming to understand the dynamics associated with shear- to extension-dominated transitions rely on further simplifications. Viscous bending stresses are often neglected throughout the entire domain (e.g., Robison and others, 2010; Pegler and Worster, 2013). Such an approximation is valid for both pure shearing (Huppert, 1982) and extentional regimes (in the latter being the only component of the stress tensor that can be formally neglected, Pietro and Cox, 1979; MacAyeal, 1989; Howell, 1996; Pegler and Worster, 2012). Nonetheless, in the vicinity of the grounding line, the vertical shear changes

significantly along the flow direction, and therefore viscous bending stresses become relevant (Pegler and Worster, 2013). Such stress gradients are known to produce swelling of a viscous flow exiting a pipe (Richardson, 1970) or downwards bending of the ice flow (Ribe, 2001; Schoof, 2011). This is also the case in our solutions under sufficiently sharp basal transitions, where the lower surface of the ice shelf does not detach from the bedrock due to the strong horizontal pressure gradient. Laboratory experiments have suggested that such an effect may cause the grounding line advance to persist for longer than estimated by models that neglect viscous bending stresses (Pegler and Worster, 2013).

Analytical results demonstrate that multiple values of Λ and q are admissible for a fixed x_{gl}, implying that equilibrium positions are not discrete. This was first hypothesized by (Hindmarsh, 1993, 1996), where the ice flux does not univocally determine the position of the grounding line, and steady marine ice sheets should be neutrally stable to changes in grounding line position. This study shows that an infinite number of pair values (Λ, q) within a certain range are compatible with a given grounding line location, forming a continuos set of equilibrium solutions. The stability of such solutions will be addressed in future work.

Upon construction of a simple ice-sheet–shelf junction, certain assumptions are necessary. Perhaps the most notable concerns the extension of a constant driving stress towards floating ice (i.e., the description of both ice sheet and ice shelf with Eq. 7). This overlooks two main points: (1) changes in driving force as grounded ice becomes afloat and (2) misalignment between the slope x-axis and the horizontal axis. In the absence of buttress, the ice shelf flow is driven by the reduced gravity $g' = g(1 - \varrho)$ (depth-integrated driving stress), differing from the slope stress with effective gravity $g' = g\,\sin\alpha$. The validity of (1) thus depends on the particular angle, yielding identical stresses for $\alpha \approx 5°$. That is, the (dimensionless) driving stress along the flow direction of a floating shelf matches that of a downwards flow of ice sloping over $\alpha \approx 5°$, supporting the assumption under a small-slope approximation. Nevertheless, even if these magnitudes are similar for the first-order problem in α, the axis misalignment would introduce a second-order contribution $g(1 - \varrho)\sin\alpha$ in the z-component of the momentum balance (Eq. 7).

For mathematical tractability, the ice flow was assumed to behave as a Newtonian fluid. However, ice exhibits a nonlinear rheology and warrants caution interpretation. The analytical results show increasing velocity gradients as the basal transition narrows, ultimately reaching a singularity for discontinuous sliding conditions. Furthermore, deviatoric stresses are not the only nonlinearity: the thermo-viscous dissipation is in fact integrably singular, revealing that ice temperatures can also modulate the solution (Nowicki and Wingham, 2008). The exact flow behaviour across the transition for a realistic nonlinear ice rheology thus

remains unknown.

CONCLUSION

This work provides analytical solutions to a classical theoretical problem in glaciology: the no-slip to free-slip glacier transition. Momentum conservation is imposed via Navier-Stokes flow with Newtonian properties under steady-state conditions. Velocity and pressure fields are smooth and well-behaved around the transition, thus overcoming difficulties found in previous studies.

Exact pressure solutions remain finite provided that the transition is continuous. On the contrary, if the basal transition presents discontinuities, the pressure diverges and becomes negatively infinite at the point-wise location of the transition. This result concludes that the asymptotic consistency of the solution only breaks down in idealised geometries with a discontinuous basal transition.

The robust mathematical treatment provides further insight on the flow structure. The changes in vorticity sign illustrate that overturning is possible, and thus the stratigraphic sequence of ice cores collected downstream can be overturned by a sufficiently sharp transition at the bed. As a result, age determination can be biased by the sliding–no-sliding zone effect, as first envisaged by Weertman (1976).

These results additionally shed light on the surface expression of acute gradients in basal conditions along the flow direction, such as glacial lakes, deformable subglacial beds, and grounding zones. Analytical solutions show that surface deflection is only present if bed friction conditions change over a horizontal scale smaller than 20% of the ice thickness.

A simple ice-sheet–shelf junction is constructed from the analytical solutions, allowing for an assessment of contact inequalities across the grounding line. A region with admissible grounding line positions is identified by exploring a range of ice flux values. These solutions satisfy both contact inequalities for multiple ice flux values, demonstrating that equilibrium positions are not discrete, but rather form a continuos set of solutions. As a result, grounding line position is not univocally determined by the ice flux under the small-slope approximation. The stability of such equilibrium solutions will be analysed in future work.

Lastly, this analytical work provides a framework for testing the accuracy and performance of numerical Stokes models in highly complex regions, where ice flow is dictated by two coexisting regimes: shear creeping and longitudinal stresses.

ACKNOWLEDGEMENTS

This research is funded by the Fonds de la Recherche Scientifique - F.R.S.-FNRS through the THAWS research project (Projet de Recherche; PDR) under Grant n° T.0234.24.

DATA AVAILABILITY

The code used to produce all results and figures is available as a persistent Zenodo repository (Moreno-Parada, 2026): `https://doi.org/10.5281/zenodo.20287174`.

REFERENCES

Bamber JL, Vaughan DG and Joughin I (2000) Widespread complex flow in the interior of the antarctic ice sheet. *Science*, **287**(5456), 1248–1250 (doi: 10.1126/science.287.5456.1248)

Barcilon V and MacAyeal DR (1993) Steady flow of a viscous ice stream across a no-slip/free-slip transition at the bed. *Journal of Glaciology*, **39**(131), 167–185, ISSN 1727-5652 (doi: 10.3189/s0022143000015811)

Barnes P, Tabor D and Walker JCF (1971) The friction and creep of polycrystalline ice. *Proceedings of the Royal Society of London. Series A, Mathematical and Physical Sciences*, **324**(1557), 127–155, ISSN 00804630

Batchelor GK (1976) *An Introduction to Fluid Dynamics*. Cambridge Mathematical Library, Cambridge University Press

Carrier G (2014) *Partial differential equations: Theory and Technique*. Academic Press, ISBN 9781483236995

Chugunov VA and Wilchinsky AV (1996) Modelling of a marine glacier and ice-sheet-ice-shelf transition zone based on asymptotic analysis. *Annals of Glaciology*, **23**, 59–67, ISSN 1727-5644 (doi: 10.3189/s0260305500013264)

Durand G, Gagliardini O, Zwinger T, Meur EL and Hindmarsh RC (2009) Full stokes modeling of marine ice sheets: influence of the grid size. *Annals of Glaciology*, **50**(52), 109–114, ISSN 1727-5644 (doi: 10.3189/172756409789624283)

England AH and Sih GC (1971) Complex variable methods in elasticity

Fowler A (2011) *Mathematical Geoscience*, volume 36 of *Interdisciplinary Applied Mathematics*, 1–872. Springer Nature

Fowler AC (1986) Sub-temperate basal sliding. *Journal of Glaciology*, **32**(110), 3–5, ISSN 1727-5652 (doi: 10.3189/s0022143000006808)

Fowler AC (2013) The motion of ice stream margins. *Journal of Fluid Mechanics*, **714**, 1–4, ISSN 1469-7645 (doi: 10.1017/jfm.2012.504)

Fowler AC and Larson DA (1978) On the flow of polythermal glaciers - i. model and preliminary analysis. *Proceedings of the Royal Society of London. A. Mathematical and Physical Sciences*, **363**(1713), 217–242, ISSN 2053-9169 (doi: 10.1098/rspa.1978.0165)

Fowler AC and Larson DA (1980) The uniqueness of steady state flows of glaciers and ice sheets. *Geophysical Journal International*, **63**(2), 333–345, ISSN 1365-246X (doi: 10.1111/j.1365-246x.1980.tb02624.x)

Gilpin R (1980) Wire regelation at low temperatures. *Journal of Colloid and Interface Science*, **77**(2), 435–448, ISSN 0021-9797 (doi: 10.1016/0021-9797(80)90314-8)

Hindmarsh RC and le Meur E (2001) Dynamical processes involved in the retreat of marine ice sheets. *Journal of Glaciology*, **47**(157), 271–282, ISSN 1727-5652 (doi: 10.3189/172756501781832269)

Hindmarsh RCA (1993) Qualitative dynamics of marine ice sheets. In *Ice in the Climate System*, 67–99, Springer Berlin Heidelberg (doi: 10.1007/978-3-642-85016-5_5)

Hindmarsh RCA (1996) Stability of ice rises and uncoupled marine ice sheets. *Annals of Glaciology*, **23**, 105–115 (doi: 10.3189/s0260305500013318)

Howell PD (1996) Models for thin viscous sheets. *European Journal of Applied Mathematics*, **7**(4), 321–343, ISSN 1469-4425 (doi: 10.1017/s0956792500002400)

Huppert HE (1982) The propagation of two-dimensional and axisymmetric viscous gravity currents over a rigid horizontal surface. *Journal of Fluid Mechanics*, **121**, 43–58, ISSN 1469-7645 (doi: 10.1017/s0022112082001797)

Hutter K and Olunloyo V (1980) On the distribution of stress and velocity in an ice strip, which is partly sliding over and partly adhering to its bed, by using a newtonian viscous approximation. *Proceedings of the Royal Society of London. A. Mathematical and Physical Sciences*, **373**(1754), 385–403

Huybrechts P and Payne T (1996) The eismint benchmarks for testing ice-sheet models. *Annals of Glaciology*, **23**, 1–12 (doi: 10.3189/S0260305500013197)

Jackson M and Kamb B (1997) The marginal shear stress of ice stream b, west antarctica. *Journal of Glaciology*, **43**(145), 415–426, ISSN 1727-5652 (doi: 10.3189/s0022143000035000)

Jacobson HP and Raymond CF (1998) Thermal effects on the location of ice stream margins. *Journal of Geophysical Research: Solid Earth*, **103**(B6), 12111–12122, ISSN 0148-0227 (doi: 10.1029/98jb00574)

Kamb B (1970) Sliding motion of glaciers: Theory and observation. *Reviews of Geophysics*, **8**(4), 673–728, ISSN 1944-9208 (doi: 10.1029/rg008i004p00673)

Kleman J and Hättestrand C (1999) Frozen-bed fennoscandian and laurentide ice sheets during the last glacial maximum. *Nature*, **402**(6757), 63–66, ISSN 1476-4687 (doi: 10.1038/47005)

Lestringant R (1994) A two-dimensional finite-element study of flow in the transition zone between an ice sheet and an ice shelf. *Annals of Glaciology*, **20**, 67–72, ISSN 1727-5644 (doi: 10.3189/1994aog20-1-67-72)

Lliboutry L (1964) *Traité de glaciologie: Glaciers, variations du climat, sols gelés*. Traité de glaciologie, Masson et Cie

Lliboutry L (1968) General theory of subglacial cavitation and sliding of temperate glaciers. *Journal of Glaciology*, **7**(49), 21–58, ISSN 1727-5652 (doi: 10.3189/s0022143000020396)

MacAyeal D (1989) Large-scale ice flow over a viscous basal sediment- Theory and application to ice stream B, Antarctica. *Journal of Geophysical Research*, **94**(B4), 4071–4087

Mantelli E and Schoof C (2019) Ice sheet flow with thermally activated sliding. part 2: the stability of subtemperate regions. *Proceedings of the Royal Society A: Mathematical, Physical and Engineering Sciences*, **475**(2231), 20190411, ISSN 1471-2946 (doi: 10.1098/rspa.2019.0411)

Mantelli E, Haseloff M and Schoof C (2019) Ice sheet flow with thermally activated sliding. part 1: the role of advection. *Proceedings of the Royal Society A: Mathematical, Physical and Engineering Sciences*, **475**(2230), 20190410, ISSN 1471-2946 (doi: 10.1098/rspa.2019.0410)

Meyer C and Minchew B (2018) Temperate ice in the shear margins of the antarctic ice sheet: Controlling processes and preliminary locations. *Earth and Planetary Science Letters*, **498**, 17–26 (doi: 10.1016/j.epsl.2018.06.028)

Meyer CR, Fernandes MC, T CT and Rice JR (2016) Effects of ice deformation on röthlisberger channels and implications for transitions in subglacial hydrology. *Journal of Glaciology*, **62**(234), 750–762, ISSN 1727-5652 (doi: 10.1017/jog.2016.65)

Moore PL, Iverson NR and Cohen D (2010) Conditions for thrust faulting in a glacier. *Journal of Geophysical Research: Earth Surface*, **115**(F2), ISSN 0148-0227 (doi: 10.1029/2009jf001307)

Moreno-Parada D (2026) Exact solutions for ice flow across the no-slip to free-slip transition (doi: 10.5281/ZENODO.20287173)

Moreno-Parada D, Robinson A, Montoya M and Alvarez-Solas J (2024) Analytical solutions for the advective–diffusive ice column in the presence of strain heating. *The Cryosphere*, **18**(9), 4215–4232, ISSN 1994-0424 (doi: 10.5194/tc-18-4215-2024)

519 Nowicki S and Wingham D (2008) Conditions for a steady ice sheet–ice shelf junction. *Earth and Planetary Science*
520 *Letters*, **265**(1-2), 246–255 (doi: 10.1016/j.epsl.2007.10.018)

521 Pattyn F (2017) Sea-level response to melting of Antarctic ice shelves on multi-centennial timescales with the fast
522 Elementary Thermomechanical Ice Sheet model (f.ETISh v1.0). *The Cryosphere*, **11**(4), 1851–1878, ISSN 1994-
523 0424 (doi: 10.5194/tc-11-1851-2017)

524 Pattyn F, De Smedt B and Souchez R (2004) Influence of subglacial vostok lake on the regional ice dynamics of
525 the antarctic ice sheet: a model study. *Journal of Glaciology*, **50**(171), 583–589, ISSN 1727-5652 (doi: 10.3189/
526 172756504781829765)

527 Pegler SS and Worster MG (2012) Dynamics of a viscous layer flowing radially over an inviscid ocean. *Journal of*
528 *Fluid Mechanics*, **696**, 152–174, ISSN 1469-7645 (doi: 10.1017/jfm.2012.21)

529 Pegler SS and Worster MG (2013) An experimental and theoretical study of the dynamics of grounding lines. *Journal*
530 *of Fluid Mechanics*, **728**, 5–28, ISSN 1469-7645 (doi: 10.1017/jfm.2013.269)

531 Perol T and Rice JR (2015) Shear heating and weakening of the margins of west antarctic ice streams. *Geophysical*
532 *Research Letters*, **42**(9), 3406–3413 (doi: 10.1002/2015gl063638)

533 Pietro NDD and Cox RG (1979) The spreading of a very viscous liquid on a quiescent water surface. *The Quarterly*
534 *Journal of Mechanics and Applied Mathematics*, **32**(4), 355–381, ISSN 1464-3855 (doi: 10.1093/qjmam/32.4.355)

535 Pollard D and DeConto RM (2009) Modelling west antarctic ice sheet growth and collapse through the past five
536 million years. *Nature*, **458**(7236), 329–332, ISSN 1476-4687 (doi: 10.1038/nature07809)

537 Pollard D and DeConto RM (2012) A simple inverse method for the distribution of basal sliding coefficients under
538 ice sheets, applied to antarctica. *The Cryosphere*, **6**(5), 953–971, ISSN 1994-0424 (doi: 10.5194/tc-6-953-2012)

539 Pritchard HD, Ligtenberg SRM, Fricker HA, Vaughan DG, van den Broeke MR and Padman L (2012) Antarctic
540 ice-sheet loss driven by basal melting of ice shelves. *Nature*, **484**(7395), 502–505, ISSN 1476-4687 (doi: 10.1038/
541 nature10968)

542 Raraty LE and Tabor D (1958) The adhesion and strength properties of ice. *Proceedings of the Royal Society of*
543 *London. Series A. Mathematical and Physical Sciences*, **245**(1241), 184–201, ISSN 2053-9169 (doi: 10.1098/rspa.
544 1958.0076)

545 Raymond C (1996) Shear margins in glaciers and ice sheets. *Journal of Glaciology*, **42**(140), 90–102, ISSN 1727-5652
546 (doi: 10.3189/s0022143000030550)

Ribe NM (2001) Bending and stretching of thin viscous sheets. *Journal of Fluid Mechanics*, **433**, 135–160, ISSN 1469-7645 (doi: 10.1017/s0022112000003360)

Richardson S (1970) A 'stick-slip' problem related to the motion of a free jet at low reynolds numbers. *Mathematical Proceedings of the Cambridge Philosophical Society*, **67**(2), 477–489, ISSN 1469-8064 (doi: 10.1017/s0305004100045758)

Rignot E, Mouginot J, Scheuchl B, van den Broeke M, van Wessem MJ and Morlighem M (2019) Four decades of Antarctic Ice Sheet mass balance from 1979–2017. *Proceedings of the National Academy of Sciences*, **116**(4), 1095–1103, ISSN 1091-6490 (doi: 10.1073/pnas.1812883116)

Robin Gd (1976) Is the basal ice of a temperate glacier at the pressure melting point? *Journal of Glaciology*, **16**(74), 183–196, ISSN 1727-5652 (doi: 10.3189/s002214300003152x)

Robison RAV, Huppert HE and Worster MG (2010) Dynamics of viscous grounding lines. *Journal of Fluid Mechanics*, **648**, 363–380, ISSN 1469-7645 (doi: 10.1017/s0022112009993119)

Schoof C (2004) Bed topography and surges in ice streams. *Geophysical Research Letters*, **31**(6), n/a–n/a (doi: 10.1029/2003gl018807)

Schoof C (2007a) Ice sheet grounding line dynamics: Steady states, stability, and hysteresis. *J. Geophys. Res*, **112**(10.1029)

Schoof C (2007b) Marine ice-sheet dynamics. part 1. the case of rapid sliding. *Journal of Fluid Mechanics*, **573**, 27–55, ISSN 1469-7645 (doi: 10.1017/s0022112006003570)

Schoof C (2011) Marine ice sheet dynamics. part 2. a stokes flow contact problem. *Journal of Fluid Mechanics*, **679**, 122–155 (doi: 10.1017/jfm.2011.129)

Schoof C (2012) Thermally driven migration of ice-stream shear margins. *Journal of Fluid Mechanics*, **712**, 552–578, ISSN 1469-7645 (doi: 10.1017/jfm.2012.438)

Schoof C and Hewitt I (2013) Ice-sheet dynamics. *Annual Review of Fluid Mechanics*, **45**(1), 217–239, ISSN 1545-4479 (doi: 10.1146/annurev-fluid-011212-140632)

Shreve RL (1984) Glacier sliding at subfreezing temperatures. *Journal of Glaciology*, **30**(106), 341–347, ISSN 1727-5652 (doi: 10.3189/s0022143000006195)

Suckale J, Platt JD, Perol T and Rice JR (2014) Deformation-induced melting in the margins of the west antarctic ice streams. *Journal of Geophysical Research: Earth Surface*, **119**(5), 1004–1025 (doi: 10.1002/2013jf003008)

Telford JW and Turner JS (1963) The motion of a wire through ice. *Philosophical Magazine*, **8**(87), 527–531, ISSN 0031-8086 (doi: 10.1080/14786436308211151)

Weertman J (1974) Stability of the Junction of an Ice Sheet and an Ice Shelf. *Journal of Glaciology*, **13**(67), 3–11 (doi: 10.3189/s0022143000023327)

Weertman J (1976) Sliding-no sliding zone effect and age determination of ice cores. *Quaternary Research*, **6**(2), 203–207, ISSN 1096-0287 (doi: 10.1016/0033-5894(76)90050-8)

Wilchinsky A and Chugunov V (2001) Modelling ice flow in various glacier zones. *Journal of Applied Mathematics and Mechanics*, **65**(3), 479–493, ISSN 0021-8928 (doi: 10.1016/s0021-8928(01)00054-5)

APPENDIX A: FOURIER COEFFICIENTS.

The solution of the problem after transformation via change of variables must satisfy all boundary conditions. In the x-axis, the conditions are straightforward and lead to an expansion in terms of the eigenfunctions $\sin(\lambda_n x)$, with the corresponding eigenvalues $\lambda_n = n\pi/L$.

There are four additional boundary conditions along the z-axis that will uniquely determine the four unknown series coefficients A_n, B_n, C_n and D_n (Fig. 2). Plugging Eq. 24 in the solution, a linear system of equations is obtained for each n, which can be simply written as:

$$\begin{pmatrix} 1 & 1 & 0 & 0 \\ \lambda_n & -\lambda_n & 1 & 1 \\ e^{\lambda_n} & e^{-\lambda_n} & e^{\lambda_n} & e^{-\lambda_n} \\ \lambda_n e^{\lambda_n} & \lambda_n e^{-\lambda_n} & e^{\lambda_n}(2+\lambda_n) & -e^{-\lambda_n}(2-\lambda_n) \end{pmatrix} \begin{pmatrix} A_n \\ B_n \\ C_n \\ D_n \end{pmatrix} = \begin{pmatrix} 0 \\ F_n \\ 0 \\ 0 \end{pmatrix} \tag{34}$$

where $F_n = \frac{1}{L}\int_0^L \tilde{f}(x,\Lambda)\,\sin(\lambda_n x)dx$ and $\tilde{f} = f(x,\Lambda) - ax/L$.

The liner system can be directly solved by Gaussian elimination without numerical solvers. The coefficients thus read:

$$A_n = F_n\left[\frac{1}{e^{-2\lambda_n}-1} + \frac{1}{e^{-2\lambda_n}(1-\lambda_n)+1}\right], \tag{35}$$

$$B_n = -A_n, \tag{36}$$

$$C_n = F_n\left[1 - \frac{1}{e^{-2\lambda_n}(1-\lambda_n)+1}\right], \tag{37}$$

$$D_n = \frac{F_n}{e^{-2\lambda_n}(1-\lambda_n)+1}. \tag{38}$$

Integrating F_n by parts, one arrives to:

$$F_n = \frac{1}{\lambda_n L}\int_0^L f_x(x,\Lambda)\,\cos(\lambda_n x)dx. \tag{39}$$

where boundary terms are cancelled by the term $-ax/L$.

For non-zero Λ, the sigmoid derivative is positive and has a global maximum, so the integral for F_n can be bounded:

$$F_n \leqslant \frac{C}{\lambda_n L}\int_0^L \cos(\lambda_n x)dx = \frac{CL}{(n\pi)^2}\,\sin(n\pi) = 0. \tag{40}$$

for some positive constant C.

On the contrary, the sigmoid function controlling the basal transition is equivalent to a step function in the limit $\Lambda \to 0$, thus simplifying the integral for F_n as $f_x(x)$ becomes a Dirac delta function centred at the transition $\delta(x - L/2)$:

$$F_n = \frac{a}{n\pi}\,\cos\left(\frac{n\pi}{2}\right). \tag{41}$$

This analytical expression permits to evaluate the convergence behaviour of the pressure field in the limit of a discontinuous basal transition.